Low-temperature phase diagrams: non-linearities due to quantum mechanical saturation of order parameters

1998 J. Phys.: Condens. Matter 10 1421

(http://iopscience.iop.org/0953-8984/10/6/025)

J. Phys.: Condens. Matter **10** (1998) 1421–1430. Printed in the UK PII: S0953-8984(98)86734-9

Low-temperature phase diagrams: non-linearities due to quantum mechanical saturation of order parameters

S A Hayward† and E K H Salje

Department of Earth Sciences, University of Cambridge, Downing Street, Cambridge CB2 3EQ, UK

Received 8 August 1997, in final form 5 November 1997

Abstract. At low temperatures, the behaviour of structural phase transitions is modified by the influence of quantum fluctuations. Such fluctuations enhance the stability of the high-symmetry phase, reducing the observed transition temperature.

The effect on phase diagrams of temperature versus some other control parameter (e.g. pressure or chemical composition) is described. A simple low-temperature extension of Landau theory is used, where the extent of quantum mechanical effects is characterized by a saturation temperature θ_S. The theory is used to model the phase diagrams of the mineral anorthoclase ($\theta_S = 271$ K), the ferroelectric materials KH_2PO_4 ($\theta_S = 49$ K), $SrTiO_3$ ($\theta_S = 20$ K for the 20 K transition), $KTaO_3$ ($\theta_S = 20$ K) and SbSI ($\theta_S = 0$ K). The saturation temperature θ_S is related to the extent to which changes in the hard phonon modes influence the transition mechanism.

1. Introduction

The thermodynamic stability of material phases at low temperatures needs special consideration, because the third law of thermodynamics implies that the entropy change at absolute zero temperature is zero. For structural phase transitions, this requirement leads to the quantum saturation of order parameters [1, 2]. Quantum saturation affects the variation of the order parameters with temperature, but not with the other variables which may control the phase transition. For pressure or external fields conjugated to the order parameter, the value zero is essentially arbitrary; there is no fundamental physical principle which forbids positive or negative values, or which requires changes in their effect on the transition. Chemical composition behaves somewhat differently. Pure endmembers can be defined in a meaningful way, and very dilute solid solutions may behave anomalously. This effect is related to the finite volume of material which any individual solute atom affects [3].

The temperature at which a structural phase transition occurs is a function of the other control parameters. We therefore have to consider the situation where the other control parameters drive the transition temperature down to temperatures where quantum saturation effects are significant. In such situations, we have the question of what a phase diagram (e.g. temperature (T) against pressure (p) or composition (x)) looks like. This is significant technologically, since many useful material properties are enhanced in the vicinity of a suitable phase transition (e.g. ferroelectrics such as PZT). These effects also have geological applications in the modelling of the thermodynamic stability of minerals.

† E-mail address: sah21@esc.cam.ac.uk

0953-8984/98/061421+10$19.50

The Clausius–Clapeyron equation determines the gradient of a (pressure–temperature) phase diagram where the differences in entropy and volume between two phases are known:

$$\frac{\mathrm{d}P}{\mathrm{d}T} = \frac{\Delta S}{\Delta V}. \tag{1.1}$$

In the classical limit, ΔS is frequently proportional to ΔV, and then the transition temperature is a linear function of pressure. However, at low temperatures $T_C(p)$ and $T_C(x)$ are often strongly non-linear, as shown below. From this, we may conclude that the ratio $\Delta S/\Delta V$ is temperature dependent, as the third law of thermodynamics predicts.

Earlier quantum mechanical calculations [4] have shown that the transition temperature T_C depends on an applied interaction S, according to the equation

$$\begin{aligned} &T_C \propto (S - S_C) && \text{in the classical limit} \\ &T_C \propto (S - S_C)^{1/2} && \text{in the quantum mechanical limit} \end{aligned} \tag{1.2}$$

where S could be (for example) pressure or chemical composition. These calculations describe the two limiting cases, but do not explain the behaviour of the crossover between the two regimes. The model is also rather difficult to incorporate into systems where several different phase transitions interact.

In this paper, we describe how the Landau theory of phase transitions can be used to determine phase diagrams, and how the incorporation of quantum mechanical effects correctly predicts the anomalies seen in phase diagrams at low temperatures. This approach is then applied to several systems of geological or technological importance.

2. Theory

Our starting point is the Landau theory of phase transitions [5] which has been used to model the thermodynamic behaviour of a number of mineral systems ([6–8] and references therein). Its classical form,

$$G = \frac{A}{2}(T - T_C)Q^2 + \frac{B}{4}Q^4 + \frac{C}{6}Q^6 + \cdots \tag{2.1}$$

is not expected to be valid at low temperatures, due to the third law of thermodynamics. To take account of these effects, it is sufficient to modify the quadratic term in equation (2.1) [1]. The resulting potential is

$$G = \frac{A\theta_S}{2}\left(\coth\left(\frac{\theta_S}{T}\right) - \coth\left(\frac{\theta_S}{T_C}\right)\right)Q^2 + \frac{B}{4}Q^4 + \frac{C}{6}Q^6 + \cdots \tag{2.2}$$

where θ_S characterizes the temperature of the crossover between classical and quantum mechanical behaviour. Typically, a phase transition behaves classically for $T > 3\theta_S/2$, and is totally saturated (the order parameter is independent of temperature) for $T < \theta_S/2$.

Equation (2.2) is exact in the displacive limit; in this case θ_S is a function of the bare soft-mode frequency [1]. For other phase transitions, there is (strictly speaking) no analytical solution for G. However, equation (2.2) has been found to be a good approximation for the solution of the self-consistency equations [2]. Furthermore, the saturation temperature θ_S has found to be correlated to the Einstein temperature θ_E by $\theta_S \approx \theta_E/2$. The full theoretical treatment of phase transitions involving many phonons will be published separately; for the purpose of this paper, θ_S can be viewed as an empirical measure of the temperature below which the temperature dependence of the order parameter is dominated by quantum mechanical effects.

In order to model the phase diagram of a material, it is necessary to consider how the coefficients in equation (2.2) will be affected by changes in pressure or chemical composition. One of the attractive features of the Landau theory of phase transitions is that this is easily accomplished, using the idea of order parameter coupling.

Provided the main effect of changing pressure is the energy due to the excess volume, the energy associated with an applied pressure will be proportional to pQ^2 in the harmonic approximation. Similarly, the energy associated with a solid solution is proportional to xQ^2, where x is the variable composition parameter, proportional to composition unless the solid solution is very dilute. An analogous argument applies to the effect of a uniaxial stress; where the spontaneous strain $\varepsilon_S \propto Q^2$, the energy effect of an applied stress is σQ^2. The total free energy of a phase transition as a function of temperature and one of these other interactions (x) is then

$$G = \frac{A\theta_S}{2}\left(\coth\left(\frac{\theta_S}{T}\right) - \coth\left(\frac{\theta_S}{T_C}\right)\right)Q^2 + \frac{B}{4}Q^4 + \frac{C}{6}Q^6 + \frac{A\theta_S k}{2}xQ^2 \tag{2.3}$$

where the interaction between Q and x does not vary strongly with temperature.

Equation (2.3) can be used to determine the equation of the phase boundary. For a second order ($B > 0$, $C = 0$) or tricritical ($B = 0$, $C > 0$) transition, the transition point will be when the Q^2 prefactor is zero:

$$\coth\left(\frac{\theta_S}{T}\right) - \coth\left(\frac{\theta_S}{T_C}\right) + kx = 0 \tag{2.4}$$

so

$$T_C^*(p, x) = \frac{\theta_S}{\coth^{-1}\left(\coth\left(\theta_S/T_C\right) - kx\right)}. \tag{2.5}$$

Figure 1 shows the difference between the classical and quantum mechanical models for a temperature–composition phase diagram. Figure 1 also shows the plateau observed for dilute solid solutions [3, 9, 10].

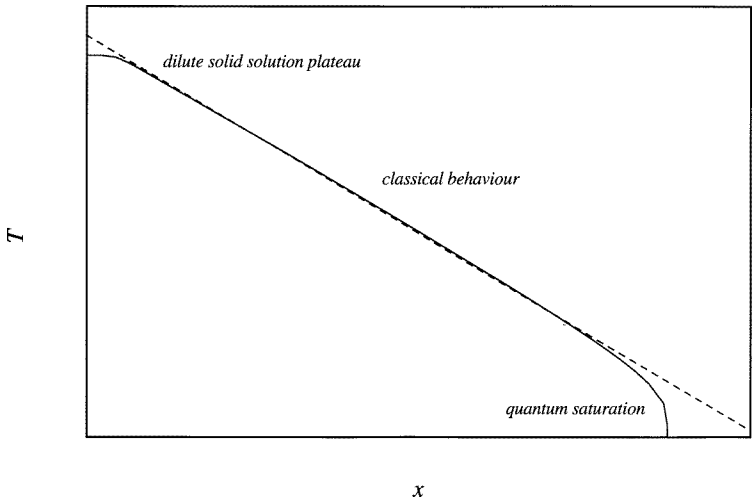

Figure 1. Composition–temperature phase diagrams predicted by the classical (broken line) and quantized (solid line) Landau potentials.

One approach to understanding why the free energy expression in equation (2.3) works is to consider the free energy of the material as the sum of the energies of the various

phonons in the structure. Using this method equation (2.3) follows directly from the soft-phonon-mode model of phase transitions [11]. If a structure contains a large number of high-frequency hard phonon modes, those modes will individually saturate at relatively high temperatures; the zero-point energy will be large compared to the thermal energy. If those modes are coupled to the order parameter, order parameter saturation will set in at a high temperature, leading to a significant non-linearity in the phase diagram. If, on the other hand, the hard modes are not a significant driving force for the transition then the saturation of the order parameter will depend solely on the soft-mode frequency. Near the transition temperature, this will be low, and so the anomaly in the phase diagram will be rather small.

3. Example phase diagrams

3.1. Anorthoclase

Anorthoclase is a solid solution between two endmembers in the feldspar group of minerals: analbite ($NaSi_3AlO_8$) and sanidine (KSi_3AlO_8), where Si and Al are fully disordered within the tetrahedral sites. Anorthoclase undergoes a displacive transition ($C2/m \leftrightarrow C\bar{1}$) which is hindered by the replacement of Na by K. Feldspar is a major component in igneous rocks, and has been widely studied (e.g. [12,13]). To complement a detailed study of the Na rich end of the solid solution [9], the (T, x) phase diagram around $Na_{0.6}K_{0.4}Si_3AlO_8$ has been determined, and is shown in figure 2.

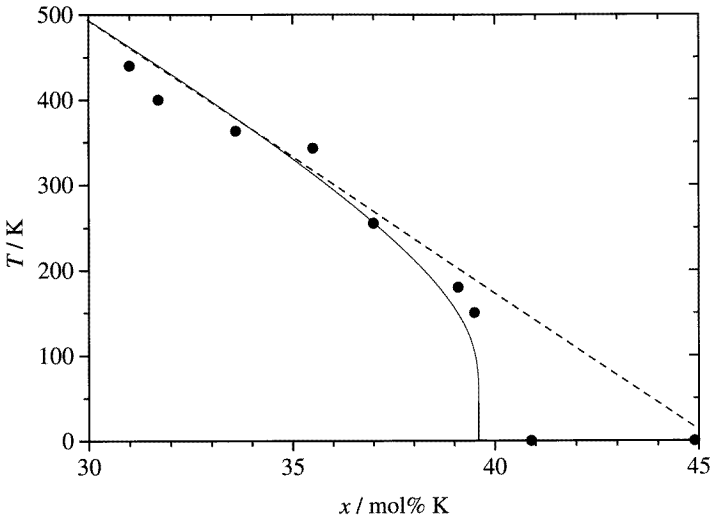

Figure 2. Experimental phase diagram for anorthoclase. The broken line shows an extrapolation of the behaviour of more Na rich samples. The solid line shows the model in equation (2.5), with $\theta_S = 271$ K.

The saturation temperature determined by fitting the experimental points in figure 2 is 271 K. This is similar to the value obtained by fitting the temperature dependence of the order parameter for pure analbite ($\theta_S = 268$ K). θ_S is expected to have some composition dependence: the hard-mode frequencies do show some variation with composition, as measured by infrared spectroscopy [14]. However such changes are too small to measure by this method. Comparison can also be made with the thermodynamic Einstein temperature

of feldspar, which is in the range 550–580 K [15], approximately twice the saturation temperature θ_S obtained here.

3.2. KH_2PO_4

Potassium di-hydrogen phosphate is an extensively studied ferroelectric material (e.g. [16–19]). It undergoes a phase transition between paraelectric ($I\bar{4}2d$) and ferroelectric ($Fdd2$) phases at 122 K at room pressure. This transition is related to the orientation of the O–H–O bonds, which link the PO_4 groups. Thermodynamically, the transition is close to the displacive limit and nearly tricritical [18].

The ferroelectric phase transition has been studied at high pressure [16, 19]. Both these studies found a linear phase boundary at low pressures, with a significant deviation at higher pressures, where the transition temperature is lower. Figure 3 shows that these data fit the quantum entropy model well; $\theta_S = 49$ K.

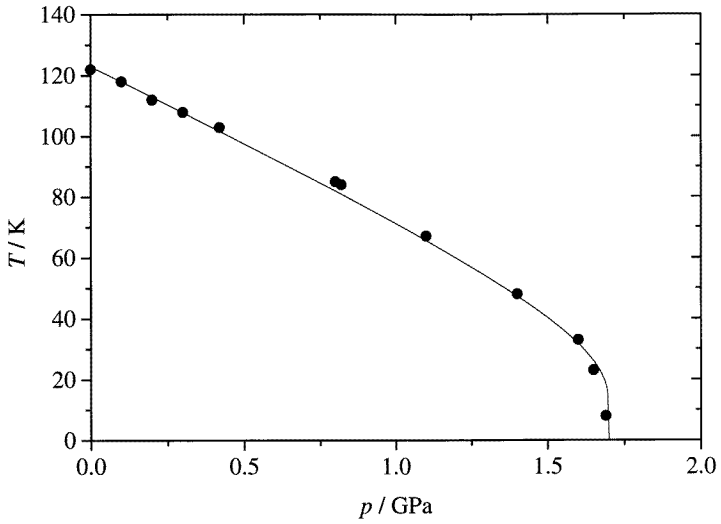

Figure 3. Phase diagram for KH_2PO_4. Data from Samara [16] and Nelmes *et al* [19] shows saturation with $\theta_S = 49$ K.

3.3. $SrTiO_3$

Strontium titanate undergoes two phase transitions on cooling from room temperature. Under ambient conditions $SrTiO_3$ has the cubic perovskite aristotype structure. Below 103 K, the octahedra rotate around the [001] axis, reducing the symmetry to $I4/mcm$.

At lower temperatures, a paraelectric–ferroelectric transition, which involves the off-centring of the Sr and Ti cations, is expected. By analogy with $PbTiO_3$, this transition would be expected to occur above absolute zero kelvin at zero pressure, but $SrTiO_3$ is paraelectric at all temperatures [20]. Later measurements [21, 22] showed that the ferroelectric phase was stabilized by applying a uniaxial stress. The stress–temperature phase diagram was determined [23] and is shown in figure 4.

The quantum saturation parameter $\theta_S = 20$ K for the ferroelectric transition in $SrTiO_3$. The extrapolated transition temperature at zero stress is 6 K, but complete saturation of

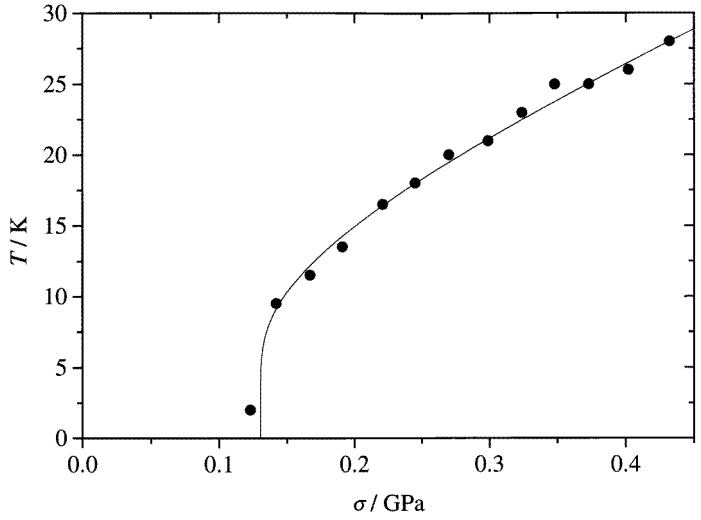

Figure 4. Stress–temperature phase diagram for $SrTiO_3$, (data from Fujii *et al* [23]). The saturation temperature is 20 K.

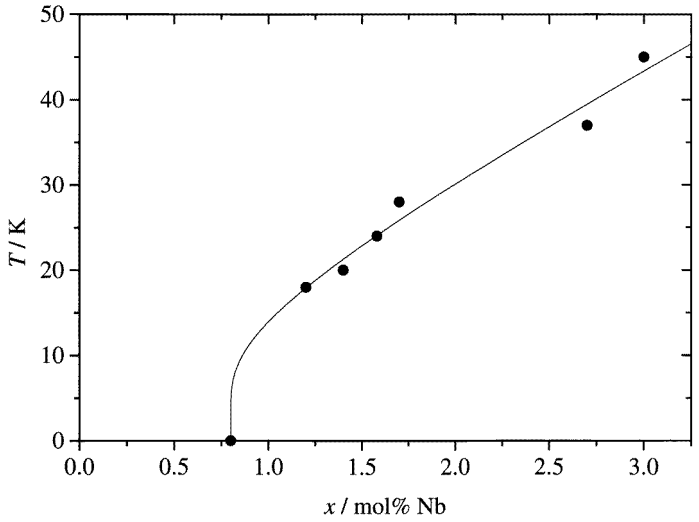

Figure 5. Composition–temperature phase diagram for $KTa_{1-x}Nb_xO_3$, showing data from Rytz *et al* [24], and a fit with $\theta_S = 20$ K.

the phase transition occurs around 10 K. As a result, the paraelectric phase is stabilized by quantum fluctuations.

3.4. $KTaO_3$

$KTaO_3$, like $SrTiO_3$, has a perovskite structure. Although pure $KTaO_3$ is paraelectric at all temperatures, a ferroelectric phase transition is observed following either of the substitutions Nb ↔ Ta or Na ↔ K. The experimental phase diagrams [24] are shown in figures 5 and 6. The (Nb, Ta) substitution on the octahedral cation site affects the ferroelectric transition

temperature much more strongly than the substitution of Na for K. This difference does not appear to affect the value of θ_S. The phase diagrams for both limbs of the solid solution give $\theta_S = 20$ K.

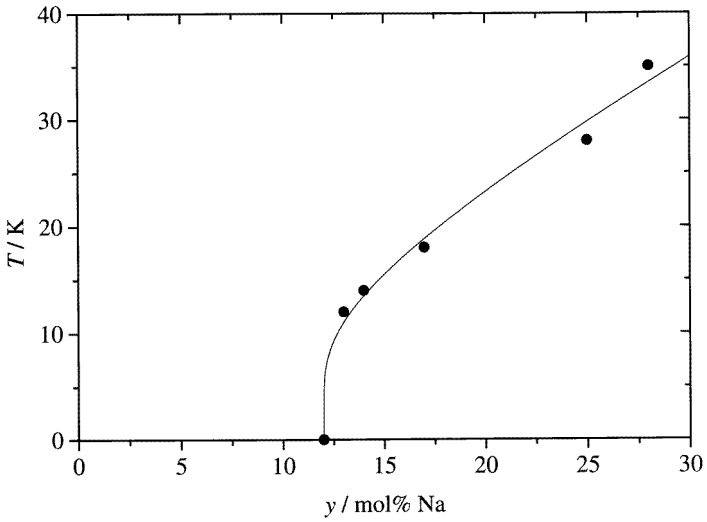

Figure 6. Composition–temperature phase diagram for $K_{1-y}Na_yTaNbO_3$. Data from Rytz *et al* [24] indicate $\theta_S = 20$ K.

3.5. SbSI

Antinomy sulpho-iodide undergoes a tricritical ferroelectric phase transition near room temperature at ambient pressure. The transition involves the displacement of S and Sb along the c axis. There is very strong coupling between the electrical and volume effects of this transition, making the material strongly piezoelectric. Another consequence of this behaviour is that the phase boundary in (p, T) space [25] is extremely steep (see figure 7).

There is no bending in the phase boundary of the type seen in the other systems studied. In other words, at the transition point, θ_S is close to 0 K. The deviations from linearity at the high-pressure end of the phase diagram probably occur because the approximation $\Delta V \propto Q^2$ is only true as a harmonic approximation: as pressure is increased, higher-order terms must also be considered.

4. Discussion

In using the equations (2.3) and (2.5) to describe these phase transitions, we have made the following assumptions:

(a) Composition is essentially homogeneous throughout the material.

(b) All the pressure effects are in the $p\Delta V$ term, rather than the other coefficients being pressure dependent.

(c) $\Delta V \propto Q^2$.

(d) θ_S is independent of p, σ and x.

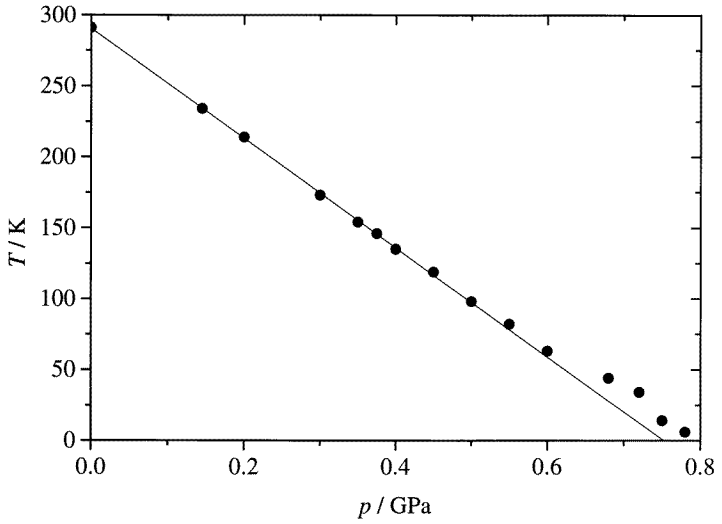

Figure 7. Pressure–temperature phase diagram for SbSI (data from Samara [25]). No quantum saturation effect is observed in the phase diagram.

The first of these assumptions is only relevant for the cases where a temperature–composition phase diagram is used. On the length scale and with the sensitivity of the experimental methods used, this assumption works well: the transition happens sharply at a well defined temperature.

The fact that the classical parts of the pressure–temperature phase diagrams are linear is good evidence for the second and third assumptions being generally applicable. SbSI appears to be a case where anharmonic volume effects are significant. However, this effect is only seen because θ_S is apparently zero.

The fourth assumption is approximately true for anorthoclase, KH_2PO_4, $SrTiO_3$ and $KTaO_3$, but totally incorrect for SbSI. The behaviour of θ_S reflects the hardness of the phonon modes driving the transition. In SbSI, the behaviour of the phase transition appears to be determined by the soft mode alone. θ_S is determined by the bare frequency of the soft mode, which goes to zero as T_C goes to zero. Thus at the low-temperature end of the phase diagram θ_S disappears, and so no anomaly is seen in the phase diagram.

Table 1 summarizes the values of θ_S obtained for various materials. In all cases examined, there is good agreement between the experimental phase diagram and the predictions of the modified Landau potential.

Some interpretation of the variation in θ_S can be made in terms of the crystal structures of the materials studied. θ_S is largest in the framework silicate minerals: anorthoclase, anorthite and quartz. This is due to the importance of the SiO_4 tetrahedron as the basic unit in the frameworks of all these structures. These tetrahedra are extremely stiff, and so vibrations which involve distortions of the tetrahedra have very high frequencies. Framework silicates therefore have a large number of hard phonon modes, which saturate at relatively high temperatures.

The fact that θ_S is large also shows that these transitions are driven by excitations (e.g. soft modes) which are strongly coupled to the hard phonons. It is the hard modes which saturate at higher temperatures, and the hard-mode saturation leads to saturation of the order parameter. In SbSI, the phase transition is purely due to the soft mode [26]; no coupling to

Table 1. Values of the saturation temperature for various phase transitions. References given are for the experimental data. Materials marked [a] are analysed in this study and are based on phase diagram measurements; the analyses of materials marked [b] are from [1] and are determined by measuring the order parameter as a function of temperature.

Transition	θ_S (K)	Source
$CaAl_2Si_2O_8$	265	[27][b]
KH_2PO_4	49	[15,18][a]
$KTaO_3$	20	[24][a]
$LaAlO_3$	194	[28][b]
Mo_8O_{23}	131	[29][b]
$Na_xK_{1-x}AlSi_3O_8$	271	this study[a]
$NaNO_3$	165	[30][b]
$Pb_3(PO_4)_2$	292	[31][b]
SbSI	0	[25][a]
SiO_2 (quartz)	334	[2]
$SrTiO_3$ (20 K transition)	20	[23][a]
$SrTiO_3$ (103 K transition)	60	[32]

hard modes seems to occur, and so the saturation temperature depends on the bare soft-mode frequency.

Another significant feature of table 1 is that the θ_S values for the two different transitions in $SrTiO_3$ are very different. The most likely explanation of this is that the couplings between the various phonons and the two order parameters are not the same. The ferroelectric transition at 20 K depends on the off-centring of the Ti cations, and so is not greatly affected by distortions outside individual octahedra. Consequently, the 20 K transition is much less strongly coupled to the phonon heat bath than the 103 K transition, which involves coupled rotations of all the TiO_6 octahedra. This weaker coupling would result in a substantially lower value of θ_S.

Acknowledgments

This project is supported by NERC and the EU Network on Mineral Transformations (contract number ERB-FMRX-CT97-0108).

References

[1] Salje E K H, Wruck B and Thomas H 1991 Order-parameter saturation and low-temperature extension of Landau theory *Z. Phys.* B **82** 399–404

[2] Salje E, Wruck B and Marais S 1991 Order parameter saturation at low temperatures: numerical results for displacive and O/D systems *Ferroelectrics* **124** 185–8

[3] Salje E K H 1995 Chemical mixing and structural phase transitions: the plateau effect and oscillatory zoning near surfaces and interfaces *Eur. J. Mineral.* **7** 791–806

[4] Schneider T, Beck H and Stoll E 1976 Quantum effects in an n-component vector model for structural phase transitions *Phys. Rev.* B **13** 1123–30

[5] Landau L D and Lifshitz E M 1980 *Statistical Physics* (Oxford: Pergamon)

[6] Salje E K H 1990 *Phase Transitions in Ferroelastic and Co-elastic Crystals* (Cambridge: Cambridge University Press)

[7] Salje E K H 1992 Application of Landau theory for the analysis of phase transitions in minerals *Phys. Rep.* **215** 49–99

[8] Carpenter M A 1992 Thermodynamics of phase transitions in minerals: a macroscopic approach *The Stability of Minerals* ed G D Price and N L Ross (London: Chapman and Hall)

[9] Hayward S A and Salje E K H 1996 Displacive phase transition in anorthoclase: the 'plateau effect' and the effect of T1–T2 ordering on the transition temperature *Am. Mineral.* **81** 1332–6
[10] Redfern S A T and Schofield P F 1996 Order parameter saturation (plateau effect) as a function of composition in the sanmartinite ($ZnWO_4$)–cuproscheelite ($CuWO_4$) solid solution *Phase Transitions* **59** 25–38
[11] Dove M T, Giddy A P and Heine V 1992 On the application of mean-field and Landau theory to displacive phase transitions *Ferroelectrics* **136** 33–49
[12] Parsons I (ed) 1988 *Feldspars and Their Reactions* (Dordrecht: Reidel)
[13] Smith J V and Brown W L 1988 *Feldspar Minerals 1: Crystal Structures, Physical, Chemical and Microtextural Properties* 2nd edn (Berlin: Springer)
[14] Zhang M, Wruck B, Graeme-Barber A, Salje E K H and Carpenter M A 1996 Phonon spectra of alkali feldspars: phase transitions and solid solutions *Am. Mineral.* **81** 92–104
[15] Keiffer S W 1985 Heat capacity and entropy: systematic relations to lattice vibrations *Rev. Mineral.* **14** 65–126
[16] Samara G A 1971 Vanishing of the ferroelectric and antiferroelectric states in KH_2PO_4-type crystals at high pressure *Phys. Rev. Lett.* **27** 103–6
[17] Brody E M and Cummins H Z 1974 Brillouin scattering of elastic anomaly in ferroelectric KH_2PO_4 *Phys. Rev.* B **9** 179–96
[18] Bastie P and Becker P 1984 Gamma ray diffraction in the vicinity of a ferroelastic transition: application to a 'real crystal' of RbH_2PO_4 and KH_2PO_4 *J. Phys. C: Solid State Phys.* **17** 193–205
[19] Nelmes R J, McMahon M I, Piltz R O and Wright N G 1991 High-pressure neutron-diffraction studies of KH_2PO_4 type phase transitions as T_C tends to 0 K *Ferroelectrics* **124** 355–60
[20] Cowley R A 1962 Temperature dependence of a transverse optic mode in strontium titanate *Phys. Rev. Lett.* **9** 159–61
[21] Burke W J and Pressey R J 1971 Stress induced ferroelectricity in $SrTiO_3$ *Solid State Commun.* **9** 191–5
[22] Uwe H and Sakudo T 1975 Stress induced ferroelectricity and soft phonon modes in $SrTiO_3$ *J. Phys. Soc. Japan* **38** 183–9
[23] Fujii Y, Uwe H and Sakudo T 1987 Stress-induced quantum ferroelectricity in $SrTiO_3$ *J. Phys. Soc. Japan* **56** 1940–2
[24] Rytz D, Höchli U T and Bilz H 1980 Dielectric susceptibility in quantum ferroelectrics *Phys. Rev.* B **22** 359–64
[25] Samara G A 1975 Effect of pressure on the dielectric properties of and vanishing of ferroelectricity in SbSI *Ferroelectrics* **9** 209–19
[26] Samara G A and Peercy P S 1981 The study of soft mode transitions at high pressure *Solid State Physics* vol 36 (New York: Academic) pp 1–118
[27] Redfern S A T, Graeme-Barber A, Salje E K H 1988 Thermodynamics of plagioclase III: spontaneous strain at the $I\bar{1} - P\bar{1}$ phase transition in Ca-rich plagioclase *Phys. Chem. Miner.* **16** 157–63
[28] Müller K A, Berlinger W and Waldner F 1968 Characteristic structural phase transition in perovskite-type compounds *Phys. Rev. Lett.* **21** 814–17
[29] Sato M, Fujishita H, Sato S and Hoshimo S 1986 Structural transitions in Mo_8O_{23} *J. Phys. C: Solid State Phys.* **19** 3059–67
[30] Reeder R J, Redfern S A T and Salje E K H 1988 Spontaneous strain at the structural phase transition in $NaNO_3$ *Phys. Chem. Miner.* **15** 605–11
[31] Bismayer U, Salje E K H, Glazer A M and Cosier J 1986 Effect of strain induced order parameter coupling on the ferroelastic behaviour of lead phosphate arsenate *Phase Transitions* **6** 129–51
[32] Hunnefeld H, personal communication